氢气泡动态模板法制备三维多孔金膜

刘　军　李　容　肖　洁　张渺岚　刘绚艳*

(湖南化工职业技术学院制药与生物工程学院,株洲　410005)

摘要：采用氢气泡阴极沉积法成功制备了具有枝晶结构的三维分级多孔 Au 膜。本文详细研究了沉积电位、沉积时间、H_2SO_4 浓度、前驱体浓度等沉积条件对形貌的影响。由枝晶构成的三维多孔金膜(3D PGFs)也可以通过方波电位法(SWP)制备。采用扫描电子显微镜(SEM)对泡沫膜的形貌进行了表征。研究表明,由纳米簇组成的 3D PGFS 对葡萄糖无酶传感具有良好的催化活性。

关键词：金泡沫膜；枝晶；电沉积；氢气泡模板；电催化

Three Dimensional Porous Gold Film Prepared by the Hydrogen Bubble Dynamic Template

LIU Jun　LI Rong　XIAO Jie　ZHANG Miao-Lan　LIU Xuan-Yan*

(*Department of Pharmaceutical and Biological Engineering, Hunan Chemical Vocational Technology College, Zhuzhou, Hunan 412005, China*)

Abstract: Au films with three-dimensional (3D) hierarchical pores consisting of interconnected dendrite walls were successfully fabricated by a strategy of cathodic deposition utilizing the hydrogen bubble dynamic template. The deposition conditions like potential, deposition time, H_2SO_4 concentration, precursor concentrations were investigated in detail. Herein, 3D Au porous films (3D PGFs) with dendritic walls could also be prepared by square wave potential (SWP). The morphology of foam films were characterized by scanning electron microscopy (SEM). The 3D PGFs comprised of nanodendrites show good electrocatalytic activities in enzyme-free detection of glucose.

Keywords: Au foam film; dendrite; electrodeposition; hydrogen bubble template; electrocatalysis

0　Introduction

Three dimensional porous materials have attracted increasing research enthusiasm due to their potential applications in areas such as electrocatalysis[1-2], superhydrophobicity[2-3], sensors[4], and surface enhanced raman scattering (SERS)[2-5].

Considering the preparation methods of porous metals, the template-directed synthesis[6-8] and the dealloying method[9-10] are widely used in the literature.

Generally, a templating method involves multisteps like creation of a porous template, pore filling and template removal. As a terminology of corrosion science, dealloying refers to selective dissolution of the less noble metal component from an alloy, resulting in a porous skeleton of the more noble metal component.

Recently, hydrogen bubbles have been utilized as a dynamic template in electrodeposition to produce self-supported 3D micro- or nano-porous metals under highly cathodic polarization. 3D foam films of non-noble

metals, such as Cu[11-12], Sn[13], Pb[14], Mg[15] and NiCoFe[16] can be obtained with the hydrogen bubble dynamic templates. The deposited Cu foams can be further transformed either into CuO foams[17] by heating or into single noble metal foam films of Pt[18], Pd[19] and Ag[19] via galvanic replacement reactions, which is a strategy to utilize the hydrogen bubble template indirectly. Compared with other template methods, this method possesses several advantages: low cost, facile control of structure, and easy preparation. Lately, our group developed a novel one-step method to prepare gold foam films by surface rebuilding of smooth gold substrates in a blank NaOH solution utilizing the hydrogen bubble dynamic template and the redox of gold electrode under square wave potential pulses[2]. Particularly, we can fabricate 3D Au foam films from the Au electrode itself requiring no Au(Ⅲ) species in solution by this method, where the gold atoms to build the foams came from the redox of metal Au. While with precursor ions of noble metals in solution, direct electrodeposition of self-supported 3D noble monometallic foams like Au[20], Pt[21], Ag[22], Pd[23] and PdAu[24] can be obtained more quickly with the hydrogen bubble dynamic templates. Even though, there are still things that remained uncertain for the formation of single noble metal foams by electrodeposition. For example, honeycomb Pt can be fabricated using the hydrogen bubble dynamic template only with a divalent Pt(Ⅱ) salt K_2PtCl_4, rather than tetravalent Pt(Ⅳ) salts, with a relatively large concentration (50 mmol·L⁻¹) in a narrow concentration range of H_2SO_4 solutions (0.1~0.2 mol·L⁻¹)[21]. Moreover, instead of foam films, only 3D Pd nano-buds and nanodendrites were obtained on a glassy carbon substrate by the hydrogen bubble templated electrodeposition in 0.2 mol·L⁻¹ NH₄Cl + 0.01 mol·L⁻¹ PdCl₂[25]. However, Pd foam could be electrodeposited from a simple solution containing 3.75~30 mmol·L⁻¹ PdCl₂ and 1 mol·L⁻¹ H₂SO₄[23]. As far as we known, many factors like precursors category and concentration, electrolyte, acidity, deposition potential or current density, deposition time, and so on can affect the formation of metal foams. That may be the reason why direct deposition of single noble metal foam films only succeeded lately with the hydrogen dynamic templates, which is once considered to be impossible.

Most recently, we synthesized 3D noble alloy foam films of AuPt[1] and PtPd[26] utilizing the hydrogen bubble dynamic template method in H_2SO_4 solutions containing low concentration of mixed precursors. The morphology and composition of AuPt alloy foams can be controlled by adjusting the deposition conditions. Noble foam films are attractive materials and worth paying more attention. Direct deposition of mono-metal foam films like Au foams were deserved further investigations, which might also be challenging and make us thinking more. In this paper, the influence factors on the electrodeposition of 3D Au foam films are investigated in detail. The electrocatalytic performances of the prepared Au foams toward enzyme-free detection of glucose reactions are also demonstrated.

1　Experimental

1.1　Reagents

HAuCl₄·4H₂O and glucose were obtained from Sinopharm Chemical Reagent Co., Ltd. (Shanghai, China). Sulfuric acid was purchased from the Factory of Hunan Normal University. All the chemicals were of analytical grade and were used as received. Milli-Q water with a resistivity of greater than 18.3 MΩ·cm was used in the preparation of aqueous solutions. D-(+)-Glu-cose (C₆H₁₂O₆·H₂O), Na₂HPO₄·12H₂O, NaH₂PO₄·2H₂O, D-fructose, sucrose, maltose monohydrate, D-mannose, lactose were obtained from Sino-pharm Chemical Reagent Co., Ltd (Shanghai, China). L-ascorbic acid (AA) (C₆H₈O₆, 99%) was purchased from Guangdong Xilong Chemical Co., Ltd (Guangzhou, China).

1.2　Electrodeposition of 3D porous Au films

Electrochemical experiments were performed on a CHI 660C electrochemical workstation (Chenhua Instruments, Shanghai, China). A gold disk (1 mm diameter, 99.99%), a platinum foil (geometric area 1 cm²), and a saturated mercurous sulfate electrode (SMSE) were employed as the working, counter, and reference electrodes, respectively. Prior to use, the working electrode was polished with 2 000 grit carbimet paper, followed by rinsing in Millipore water under ultrasonic waves.

Then, the well-polished electrode was electrochemically pretreated by cycling the potential between −0.7 and 1.1 V in 1 mol·L⁻¹ H₂SO₄ at a scan rate of 100 mV·

s^{-1} until a stable voltammogram was obtained. Then the gold electrode was rinsed with Millipore water. The electrodeposition conditions of 3D PGFs were optimized at room temperature （~25 ℃） by varying the deposition potential （−1.5, −3, −4, −5 V）, deposition time （10, 100, 500 s）, sulfuric acid concentration （0.5, 2, 5, 10 mol·L^{-1}） and HAuCl$_4$ concentrations （0.4, 2, 5, 10 mmol·L^{-1}）. 3D PGFs with dendritic walls could be prepared by the SWP （between 1.5 and −4 V, 10 Hz） in the electrolyte of 2 mmol·L^{-1} HAuCl$_4$+2 mol·L^{-1} H$_2$SO$_4$ for 500 s. The current densities of Au foam catalysts for enzyme-free detection of glucose were normalized to the total electro-chemical active surface （EASA）, which were calculated using the double layer capacity measurements[27]. The deposited Au foam film was first treated by cyclic voltammetry between −0.70 and 1.1 V at 100 mV·s^{-1} in 1 mol·L^{-1} H$_2$SO$_4$ solution until a steady cyclic voltammo-gram （CV） was obtained. CVs of 3D porous Au film between 0.04 and 0.20 V in 1 mol·L^{-1} H$_2$SO$_4$ at 20, 50, 100, 200, 300, 400, 500 mV·s^{-1} were tested. All solutions were freshly prepared with Millipore water and analytical grade chemicals. All experiments were performed at room temperature.

1.3　Characterizations of the deposited foam films

The morphology images of the electrodeposited foam films were taken with a JEOL JSM-6360 scanning electron microscope （SEM） operating at 25 kV.

1.4　Electrooxidation of glucose

3D PGFs prepared in a solution of 2 mmol·L^{-1} HAuCl$_4$+2 mol·L^{-1} H$_2$SO$_4$ by electrodeposited along with H$_2$ evolution at constant potential of −4 V treated for 500 s, were evaluated as a glucose sensor in a 0.1 mol·L^{-1} phosphate-buffered saline （PBS） solution containing 0.1 mol·L^{-1} Na$_2$SO$_4$ as a supporting electrolyte at desired potentials. The currents in each experiment were recorded after the transient reached a steady state. Amperometric curves were obtained after adding desired concentration of glucose with the solution stirred constantly. Before measurements, 3D PGFs were electrochemically activated by using a SMSE as reference to avoid the specic adsorption of chloride ions, and obtain valid and reproducible results.

2　Results and discussion

2.1　Characterizations of the electrodeposited foam films

Fig.1 shows the time-dependent morphological evolution of 3D PGFs, which were electrodeposited at −4 V in the solution of 2 mmol·L^{-1} HAuCl$_4$+2 mol·L^{-1} H$_2$SO$_4$. The SEM images demonstrate that application of

Fig.1　SEM images of the 3D PGFs prepared in a solution of 2 mmol·L^{-1} HAuCl$_4$+2 mol·L^{-1} H$_2$SO$_4$ by electrodeposited along with H$_2$ evolution at constant potential of −4 V treated for different deposition times of (a1~a3) 10 s, (b1~b3) 100 s and (c1~c3) 500 s

different deposition times results in the different morphologies of 3D PGFs. The origin of this unique structure is discussed elsewhere and briefly summarized in the earlier report[11]. The film is too thin to form foam in short deposition time of 10 s (Fig.1(a1,a2)), there are many small dendrites on the substrate electrode (Fig. 1a3). When the deposition time is prolonged to 100 s, the 3D PGFs film reaches a certain thickness and H_2 bubbles begins to guide the formation of micropores with a diameter of 10~20 μm (Fig.1(b1,b2)). Since at this stage the film is still thin, and the formed micropore walls are highly porous because of vigorous evolution of hydrogen. The resulting self-supported porous films are micropores in the frame and nanopores in the walls, and the walls are made up of irregular gold nano-ramified structures (Fig.1b3). For the longer electrolysis time, after 500 s of electrodeposition, it is clear that the thickness and the pore size (with a diameter of 20~50 μm) of the 3D micro-foam structure increases with the time of deposition (or the distance from the Au substrate) (Fig.1(c1,c2)), and the irregular gold nano-ramified structures become more thicker and stronger because of coalescing of gold nanoparticles (Fig.1c). Such an open porous structure can facilitate fast mass transfer of gas and liquid, while the extremely high area is good for electrocatalytic reactions.

Among the deposition paremeters studies, the concentrations of the $HAuCl_4$ greatly influenced the morphologies of the foam deposition. If the concentration of $HAuCl_4$ is too low (less than 0.4 mmol·L^{-1}), the walls of Au foam become too thin to form a 3D structure (Fig. 2a). In contrast, the higher concentrations of $HAuCl_4$ than the optimum amount (2 mmol·L^{-1}) result in thicker and denser foam walls (Fig.2(b,c)). The well-defined 3D PGFs with highly open porous walls can be fabricated in a relatively wide concentration range of $AuCl_4^-$ ions (from 2 to 10 mmol·L^{-1}).

Furthermore, the H_2SO_4 concentration shows a considerable effect on the formation of 3D PGFs (Fig.3). The increase in the concentration can improve the reaction rates. Fig.3 shows SEM images of 3D PGFs grown from 2 mmol·L^{-1} $HAuCl_4$ with different concentrations of H_2SO_4 (0.5, 5 and 10 mol·L^{-1}). The thickness of Au foam increases with the electrolyte concentration within the same deposition time (Fig.(3a~c)).

For electrodeposition technique, applied potential is an important factor for controlling the morphologies of 3D PGFs. Fig.4 shows the SEM images of the 3D PGFs obtained at different electrolysis potentials at a fixed concentration (2 mmol·L^{-1} $HAuCl_4$+2 mol·L^{-1} H_2SO_4) and room temperature (~25 ℃) within 500 s. For the different electrolysis potentials, the morphologies are more or less similar, with certain differences. During the electrolysis process, the applied potentials (−1.5, −3.0 and −5.0 V) are sufficient for the reaction $AuCl_4^-$+3e=Au+4Cl^- (E= 0.339 V vs SMSE) and hydrogen evolution to take place

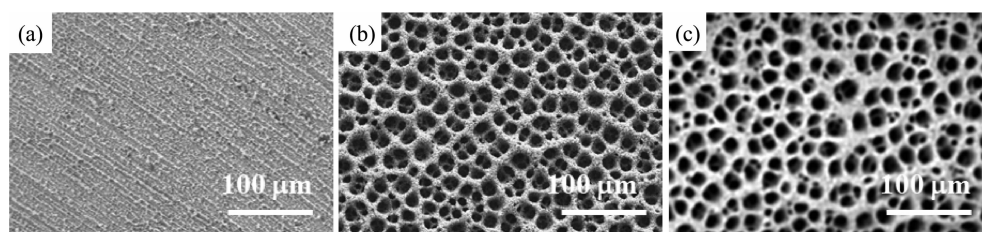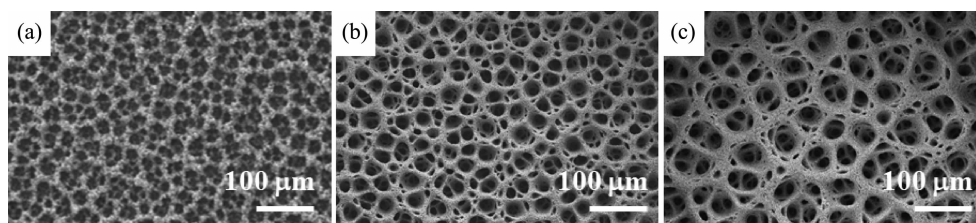Fig.2　Typical SEM images of 3D PGFs electrodeposited under constant potential electrolysis at −4 V for 100 s in the solution of 2 mol·L^{-1} H_2SO_4 containing (a) 0.4, (b) 5 and (c) 10 mmol·L^{-1} $HAuCl_4$

Fig.3　Typical SEM images of 3D PGFs electrodeposited under constant potential electrolysis at −4 V for 500 s in the solution of 2 mmol·L^{-1} $HAuCl_4$ with different H_2SO_4 concentrations of (a) 0.5, (b) 5 and (c) 10 mol·L^{-1}

on the working electrode. For the materials obtained at lower potentials (−1.5 and −3.0 V), the 3D porous Au structures were also observed (Fig.4(a,b)). For example, the morphologies shown in Fig.4a, are obtained using −1.5 V, the deposit in this case seems to consist of large pores, thin walls and the thickness of Au film is also thin. At the more negative potential of −3.0 V (Fig.4b), both the walls of 3D porous and the thickness of Au film become thicker while the diameter of pores chang a little. We expect that the fast growth rate observed at the higher potential causes the Au to fill in the gaps between the initially deposited bumps. At more negative

potential (−5.0 V), 3D porous Au structures were clearly observed (Fig.4c).

The 3D PGFs with dendritic walls could also be prepared by SWP. The morphologies of 3D PGFs prepared by SWP (−4 V~1.5, 10 Hz) are shown in Fig.5. It is clearly seen that the gold substrate is covered with a thick layer of foam microstructures with micropores, the diameter of these micropores is about 10~20 μm (Fig.5(a,b)). Further detailed examinations reveal that the pores are highly connected (Fig.5b), and the walls are composed of well-defined dendritic structures (Fig.5(c,d)).
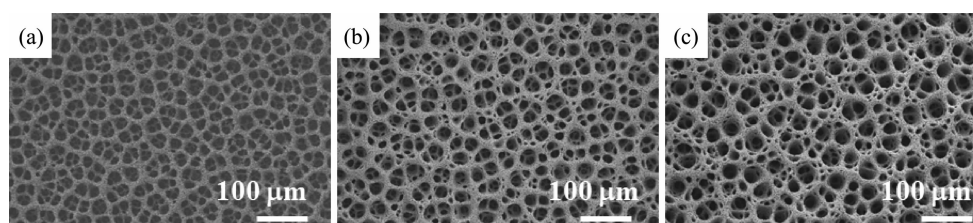

Fig.4　SEM images for the 3D PGF samples prepared by electrodeposited along with H_2 evolution in the solution of 2 mmol·L^{-1} $HAuCl_4$ + 2 mol·L^{-1} H_2SO_4 for 500 s at different potentials of (a)−1.5, (b)−3 and (c)−5 V
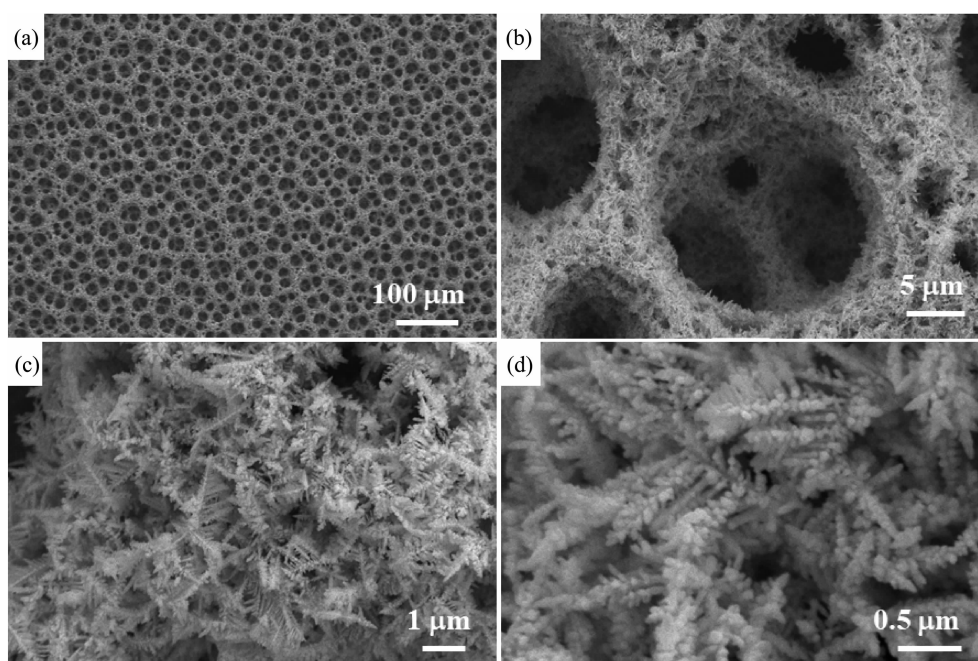

Fig.5　SEM images of the 3D PGFs with dendritic walls electrodeposited along with H_2 evolution by the SWP ((between 1.5 and − 4 V, 10 Hz) in the electrolyte of 2 mmol·L^{-1} $HAuCl_4$ + 2 mol·L^{-1} H_2SO_4 for 500 s

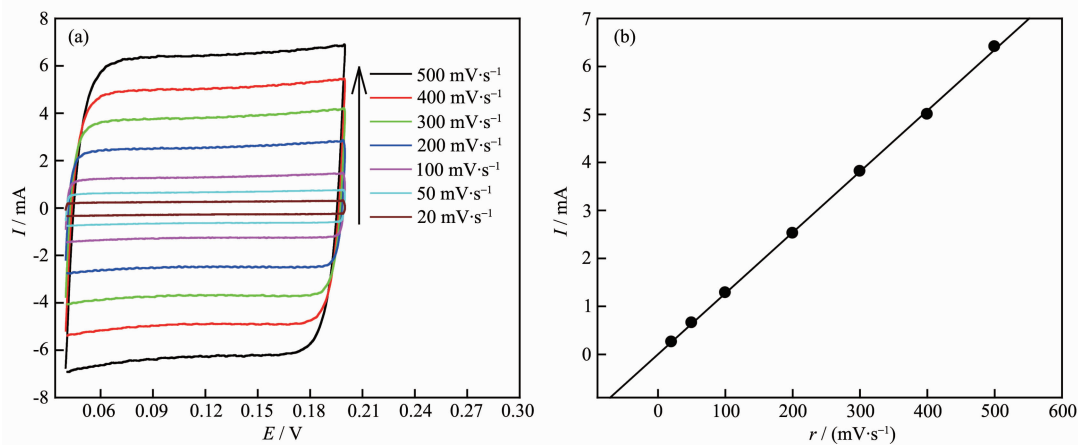## 2.2　Electrocatalytical activity of PGFs

The current densities of enzyme-free detection of glucose are normalized to the electrochemically active surface areas, which are calculated by measuring the double layer capacity measurements. Fig.6a shows

capacitive currents during the electrode polarization in the double layer region and their dependence on scan rate. Herein, the real surface area of the electrode is calculated as $S=C/C_0$. Where S is the ECSA, C is the capacity of the electrical double layer, C_0 is the capacity

per unit area. From the slope of *I-r* relationship (Fig.6b), the double layer capacity of the electrode studied is obtained. The value of 44.5 $\mu F \cdot cm^{-2}$ (in 1 $mol \cdot L^{-1}$ H_2SO_4), found for Au, is then used to calculate the real surface area of 3D porous Au foam. Herein, the ECSA of 3D porous Au is calculated as 275 cm^2.

　　3D PGFs with the interconnected macroporous walls and the high surface are considered as good catalysts in enzyme-free detection of glucose. The performance of glucose biosensors is usually tested under physiological conditions. Therefore, the electro-catalytic activity of the Au film electrode toward the oxidation of glucose was investigated in a PBS solution containing 0.1 $mol \cdot L^{-1}$ Na_2SO_4 as supporting electrolyte.

Fig.7a shows the cyclic voltammogram of the oxidation of glucose at a porous Au film electrode in a pH =7.4 PBS solution containing 0.1 $mol \cdot L^{-1}$ Na_2SO_4 and 100 $mmol \cdot L^{-1}$ glucose at 10 $mV \cdot s^{-1}$. The CV in the positive potential scan shows two anodic current peaks located at −0.55 V (I) and −0.20 V (II). The current peak (I) should be due to the electrosorption of glucose to form adsorbed intermediate, releasing one proton per glucose molecule. With the potential moving to more positive values, free Au active sites are released for the direct oxidation of glucose, and a current peak at −0.20 V for this direct oxidation appears. In the negative potential scan, with the increasing of the surface Au, enough surface active sites will be available for the direct oxidation of glucose,

3D PGFs prepared in a solution of 2 $mmol \cdot L^{-1}$ $HAuCl_4$+2 $mol \cdot L^{-1}$ H_2SO_4 by electrodeposited along with H_2 evolution at constant potential of −4 V treated for 500 s

Fig.6　(a) CVs of 3D porous Au film between 0.04 and 0.20 V in 1 $mol \cdot L^{-1}$ H_2SO_4 at different scan rates (*r*);
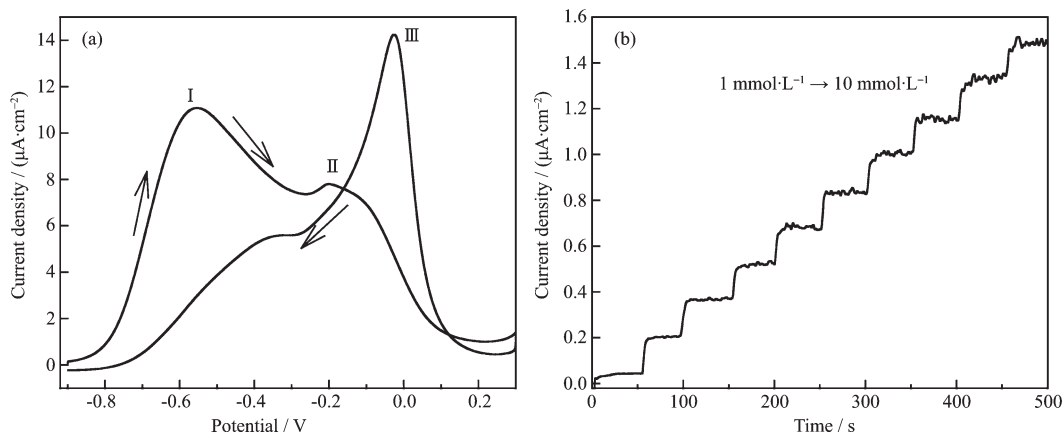(b) Slope of *I-r* relationship at 0.11 V

Fig.7　(a) CV of the 3D PGFs electrode in a solution of 0.1 $mol \cdot L^{-1}$ PBS+0.1 $mol \cdot L^{-1}$ Na_2SO_4 +100 $mmol \cdot L^{-1}$ glucose at a scan rate of 10 $mV \cdot s^{-1}$; (b) Typical amperometric response of the 3D PDFs to glucose in a stirring 0.1 $mol \cdot L^{-1}$ PBS+ 0.1 $mol \cdot L^{-1}$ Na_2SO_4 solution by successive addition of 1 $mmol \cdot L^{-1}$ glucose under the applied potential of −0.2 V versus SMSE

resulting in an anodic current peak at −0.02 V(Ⅲ).

For practical application, however, an amperometric sensor is more useful than a voltammetric one. We attempt to development a non-enzymatic glucose sensor for the glucose is an important clinical medicine biomolecule. Fig.7b shows the amperometric response of the 3D PFGs electrode, held at an optimized detection potential of −0.2 V, to the successive addition of 1 mmol·L^{-1} glucose at the points as indicated by arrow. With each addition of glucose to the stirred supporting electrolyte solution, the current rapidly increases. One can see that oxidation current linearly increases for glucose concentrations in the range of 1~10 mmol·L^{-1}.

3　Conclusions

In summary, a facile, one-step hydrogen bubble dynamic template electrodeposition method has been developed to prepare three-dimensional porous gold film (3D PGF) with highly open porous walls in a low concentration of HAuCl$_4$ (2 mmol·L^{-1}) solution. The pore diameters and wall thickness of the porous gold films can be easily controlled by varying deposition time, concentration of the precursors, supporting electrolyte, and the applied potentials. Herein, we also have developed a SWP method to prepare 3D PGFs with dendrite walls. The 3D PGFs have good catalysts in enzyme-free detection of glucose.

References:

[1] Liu J, Cao L, Huang W, et al. *ACS Appl. Mater. Interfaces*, **2011,3**:3552-3558

[2] Huang W, Wang M H, Zheng J F, et al. *J. Phys. Chem. C*, **2009,113**:1800-1805

[3] Gu C D, Xu X J, Tu J P. *J. Phys. Chem. C*, **2010,114**:13614-13619

[4] Xia Y, Huang W, Zheng J F, et al. *Biosens. Bioelectron.*, **2011,26**:3555-3561

[5] Najdovski I, Selvakannan P R, O'Mullane A P, et al. *Chem. Eur. J.*, **2011,17**:10058-10063

[6] Lu L, Eychmüller A. *Acc. Chem. Res.*, **2008,41**:244-253

[7] Jiang A N, Zhang B H, Xue Y G, et al. *Microporous Mesoporous Mater.*, **2017,248**:99-107

[8] Stephen D W, Mark A B, Patrick I H, et al. *Electrochim. Acta*, **2016,222**:361-369

[9] Geun H L, Sehoon A, Seong W J, et al. *Thin Solid Films*, **2017,631**:147-151

[10]Sun Y X, Ren Y B, Yang K. *Mater. Lett.*, **2016,165**:1-4

[11]TAN Sheng-Chun(谭盛春), JIANG Wen-Shi(江文世). *Electroplating & Finishing*(电镀与涂饰), **2012,31**(4):1-3

[12]Najdovski I, O'Mullane A P. *J. Electroanal. Chem.*, **2014,722**:95-101

[13]ZHOU Yin-Hua(周颖华), CEN Shu-Qiong(岑树琼), SHAO Yu-Tian(邵玉田), et al. *Journal of Zhejiang Normal University*(浙江师范大学学报), **2007,30**(3):307-313

[14]HAN Jin-Yu(韩金玉), ZHAO Ming-Ming(赵明明), WANG Hua(王华). *Journal of Tianjin University*(天津大学学报), **2014,47**(7):619-624

[15]Cheng G, Xu Q, Zhao X, et al. *Trans. Nonferrous Met. Soc. China*, **2013,23**:1367-1374

[16]Lidija D R, Christoph G, Christian R, et al. *Nano Energy*, **2013,2**:523-529

[17]Cherevko S, Chung C H. *Talanta*, **2010,80**:1371-1377

[18]Yin J, Jia J B, Zhu L D. *Int. J. Hydrogen Energy*, **2008,33**:7444-7447

[19]Shahbazi P, Kiani A. *Electrochim. Acta*, **2011,56**:9520-9529

[20]Cherevko S, Chung C H. *Electrochem. Commun.*, **2011,13**:16-19

[21]Ott A, Jones L A, Bhargava S K. *Electrochem. Commun.*, **2011,13**:1248-1251

[22]Cherevko S, Shin C H. *Electrochim. Acta*, **2010,55**:6383-6390

[23]Cherevko S, Kulyk N, Chung C H. *Nanoscale*, **2012,4**:103-105

[24]Liu J, Wang J, Kong F D, et al. *Catal. Commun.*, **2016,73**:22-26

[25]Yang G M, Chen X, Li J, et al. *Electrochim. Acta*, **2011,56**:6771-6778

[26]Liu J, Cao L, Huang W, et al. *J. Electroanal. Chem.*, **2012,686**:38-45

[27]Łukaszewski M, Czerwiński A. *Thin Solid Films*, **2010,518**:3680-3689